06,16

Dynamics of the electric field in a lithium niobate crystal during pyroelectric generation of electric discharges

© K.M. Mambetova[1], S.M. Shandarov[1], A.I. Aksenov[1], L.N. Orlikov[1], N.I. Burimov[1], M.A. Bryushiin[2], I.A. Sokolov[2]

[1] Tomsk State University of Control Systems and Radioelectronics, Tomsk, Russia,
[2] Ioffe Institute, St. Petersburg, Russia
E-mail: mambetova_ksenia@mail.ru

Received October 8, 2024
Revised November 12, 2024
Accepted November 13, 2024

The article presents a technique for experimentally studying the dynamics of the electric field during pyroelectrically induced generation of electric discharges in a lithium niobate crystal with parallel Z-faces, which is a Fabry-Perot resonator. Recording the intensity of the laser beam reflected from the crystal during heating and cooling cycles in an air atmosphere made it possible to detect its abrupt changes occurring over a time not exceeding $1\,\mu$s. Analysis of these changes associated with electric discharges showed that they are accompanied by a decrease in the field strength in the crystal and the surface charge, which reaches values of 4 kV/cm and 23 nC, respectively.

Keywords: pyroelectric effect, lithium niobate, Fabry-Perot interferometer, electrical discharges.

DOI: 10.61011/PSS.2024.11.60097.257

1. Introduction

The high pyroelectric properties and low conductivity of $LiNbO_3$ and $LiTaO_3$ crystals belonging to the symmetry class $3m$ are the basis for creating solid-state devices for generating fluxes of charged particles, X-rays and neutrons [1–11]. The physical mechanism of generation is associated with strong electric fields created by charges occurring on the polar faces of pyroelectric crystals in case of temperature variations. X-ray and neutron generation processes take place in the vacuum conditions [1–5,7–11], while the pyroelectric ion source for mass spectrometry described in Ref. [6] operated at atmospheric pressure. The ionization process took place in it during thermal cycling in the temperature range from 40 to 103°C of Z-cut pyroelectric crystal ($LiNbO_3$ or $LiTaO_3$) located in vapors of organic substances. At the same time, the authors of Ref. [6] believe that electrical discharges between two Z-facets of the crystal used are the main cause of ion formation. Discharges can also occur in X-ray generation devices [3,7–11] in the gap between one of the Z-faces of the pyroelectric sample and the target, on which electrons accelerated by an electric field are decelerated. Such pyroelectric generation of electric discharges shall be accompanied by a change of the total surface charge of the crystal $\Delta\xi(t)$ and a corresponding decrease of the electric field strength in the crystal and in the accelerating gap by some values $\Delta E_3^{cr}(t)$ and $\Delta E_3^{g}(t)$. The rates of change of the surface charge due to crystal heating and due to electrical discharges, which strongly depend on external conditions, significantly differ, which leads to the generation of accelerated electron fluxes in the form of sporadic pulses.

The amplitude and time characteristics of the current in the discharge pulses, as well as data on the charge carried during this process, are understudied, and the information published about them is contradictory. For example, the order of the emission current density for lithium niobate under high vacuum conditions (10^{-6} Torr) induced by the pyroelectric effect is estimated as $10^{-9}-10^{-10}$ A/cm^2 in the review in Ref. [1]. The authors of Ref. [4] obtained for congruent $LiNbO_3$ at the same pressure that pyroelectric electron emission in the cycle of cooling from 120°C realized from the face $-Z$, located at a distance of more than 2 mm from the target, is characterized by a stable current reaching a constant level of ~ 100 nA at temperatures close to room temperature. The electronic current in the gap between the surface of a lithium tantalate crystal and a copper target, with values of 11, 13 and 15 mm, was measured in Ref. [11] with a picoammeter using a protective circuit consisting of a resistor and two diodes to prevent overload during breakdown. A relatively smooth change of current from ~ 0.8 to -1 nA was recorded here for 15 mm gap over a time interval of 1500 s under conditions of medium vacuum (2 mTorr) and periodic temperature variation with a frequency of 2 MHz, with its average value of $T_0 \approx 20$°C.

The authors of Ref. [12] studied sporadic pulsed electrical discharges generated at atmospheric pressure in the cycles of heating and cooling of $LiNbO_3$ pyroelectric crystal. The crystal had a thickness of 1 mm and its polar surface

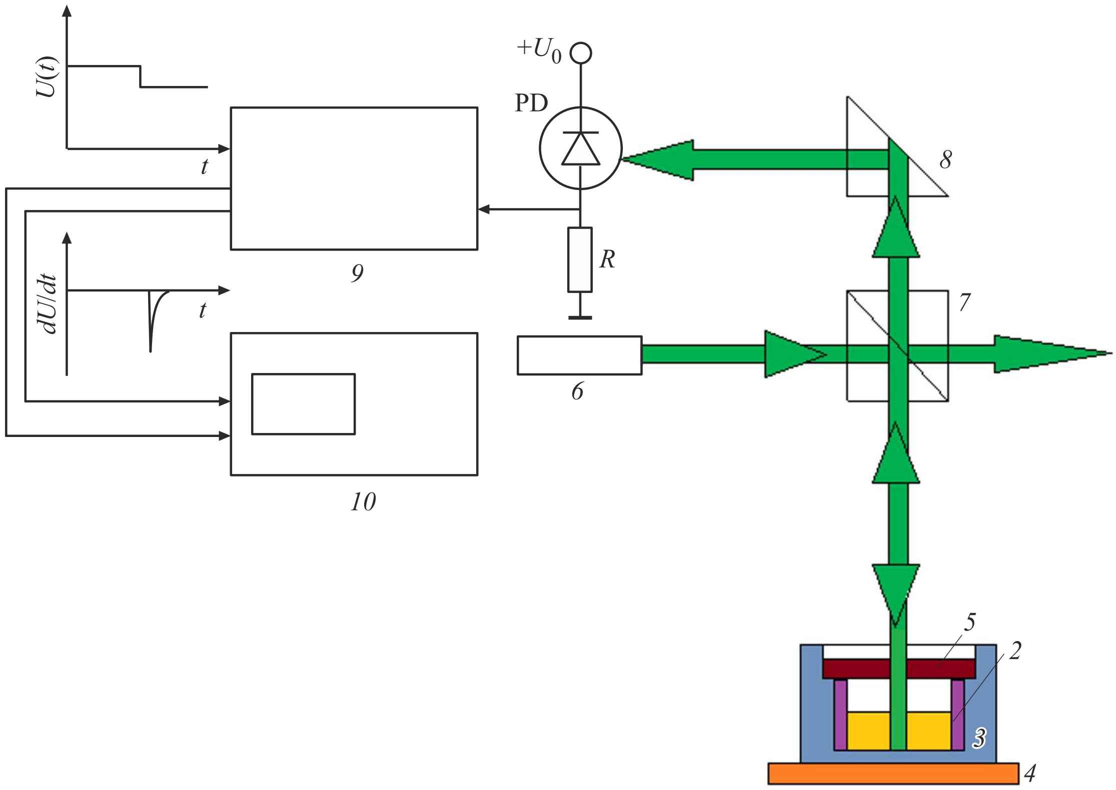

Figure 1. Experimental setup: *1* — lithium niobate crystal, *2* — dielectric insert, *3* — copper cylinder, *4* — heater, *5* — translucent anode, *6* — single-frequency laser, *7* — dividing cube, *8* — prism, *9* — optical signal processing unit, *10* — an oscilloscope.

$+Z$ was directed to a pointed tungsten electrode located at a distance of 1 mm, grounded through a picoammeter or 100 Ω resistor. In the latter case, the discharge current was measured based on the voltage across this resistor, recorded by Tektronix DPO 2024B oscilloscope with a band of 200 MHz. It was found that the amplitude of the discharge pulses reaches values not exceeding ~ 80 nA in the heating cycle and ~ 7 nA in the natural cooling cycle of the crystal, however, their time parameters were not considered in detail by the authors of this paper.

Time parameters of discharge pulses for a cylindrical pyroelectric crystal of lithium niobate at atmospheric pressure are studied in detailed in Ref. [13]. The device for measuring discharge currents between the crystal face $+Z$ and the cylindrical copper electrode (target) had a coaxial geometry that allowed matching the load resistance node (5.1, 2.55, or 1.7 Ω) with the input resistance of broadband oscilloscopes Keysight DSO-X 3102T (1 GHz) or Tektronix MSO6B (8 GHz). As a result, discharge pulses of positive/negative polarity with a rise time from 1 to 1.9 ns and a duration of ~ 15 ns were recorded in the cooling/heating cycles; the maximum currents were up to 600 mA and a transferred charge was up to 5.7 nC.

The reflection of a laser beam with a wavelength of 532 nm is used in this paper for the first time to study the dynamics of an electric field in a cylindrical lithium niobate crystal with parallel faces $Z+$ and $Z-$ in case of pyroelectric discharge generation. The reflectance from such a crystal, representing the Fabry-Perot interferometer, is determined by its refractive index, which, due to the linear electro-optical effect, depends on the electric field strength. The recording of the intensity of reflected light by a photodetector system and a two-channel digital oscilloscope in a standby mode in the sweep rate range from 10 s/div to 1 μs/div allowed observing sharp changes of the electric field strength in the crystal in the heating and cooling cycles associated with pyroelectrically induced electric discharges.

2. Experimental setup

The experimental setup is shown in Figure 1. A cylindrical crystal of lithium niobate (*1*) with a diameter of $D = 17.0$ mm and a thickness of $h_{cr} = 12.2$ mm was centered by a dielectric insert (*2*) in a hollow copper cylinder (*3*). The latter was placed on a programmer-controlled resistive heater (*4*), the temperature of which was controlled by a thermocouple and could vary in the heating cycle at a rate of up to 10 K/min in the range of up to 110°C. The rate of the heater temperature drop in the natural cooling cycle decreased from 10 K/min at temperatures of the order of 100°C to 1 K/min at temperatures below 40°C. A translucent anode (*5*) in the form of an ITO film sputtered onto a glass plate of glass with a thickness of 2 mm in contact with a copper cylinder was placed above the crystal at a distance of $h_g = 10$ mm. The changes of the crystal accompanying electrical discharges were recorded using a reflection of a laser beam with a wavelength of 532 nm from two parallel faces $Z+$ and $Z-$ of the sample, representing a Fabry-Perot optical resonator, using a laser (*6*), the dividing cube (*7*) and the prism (*8*). The time dependences of variations in the intensity of the reflected light beam were recorded using BWP34 photodiode, which was connected via an emitter repeater (*9*) to the input of a Keysight DSO-X 3102T broadband digital oscilloscope (1 GHz) (*10*). A differentiating link and a single-stage transistor amplifier were used to implement a standby scanning mode corresponding to the beginning of rapid changes in the intensity of the laser beam reflected from the crystal.

It should be noted that stability of the emitter repeater mode is required to implement a standby scanning in the experimental setup used, which was ensured by selecting its operating point corresponding to a certain nonzero voltage U_0 at the input of the oscilloscope and with no signal from the *pin*-photodiode.

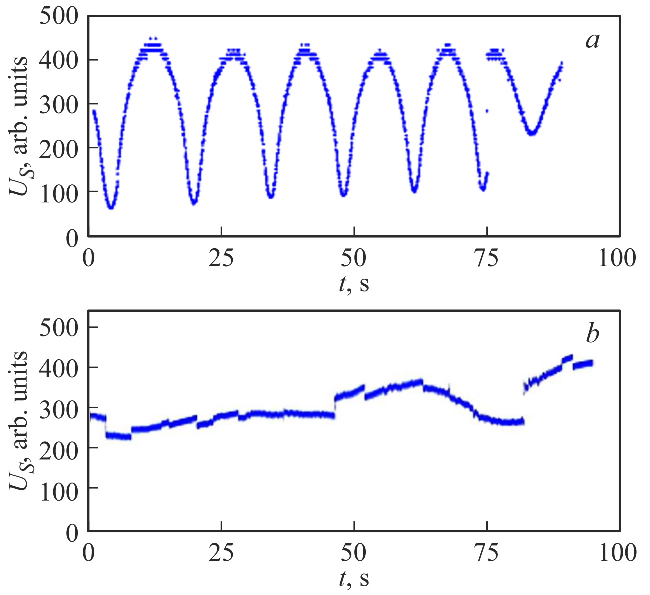

Figure 2. Time dependences of voltage recorded with a sweep rate of 10 s/div in heating (*a*) and cooling cycle (*b*).

3. Experimental results

Both slow changes of the intensity of the reflected beam $I_R(t)$, associated with the thermo-optical effect and pyroelectric induction of the electric field, and its sharp jumps were observed with variations of the crystal temperature. The results shown below in Figures 2–5 correspond to several experiments in which the heating cycle from ~ 22 to $\sim 110°$C had a duration of about 9 min, and the cooling cycle to $\sim 30°$C — more than 30 min. The time dependences of the voltage at the output of the optical signal processing unit $U_S(t)$, recorded by the oscilloscope at a sweep rate of 10 s/div in intervals of about 90 s, are shown in Figure 2. Figure 2, *a* corresponds to the crystal heating cycle for the range measured by the thermocouple from 24 to 39°C, in which two sections of a smooth change of the output signal are separated by its sharp jump at time $t = 75$ s. The oscillogram for the cooling cycle at the same sweep rate, illustrated in Figure 2, *b* for a small temperature range, from 42 to 40°C, contains more than 15 sharp changes of the output voltage.

As noted earlier, $U_S(t)$ contains a constant component U_0 associated with the choice of the emitter repeater operating point. The variable component of the signal $U_{FP}(t)$ displays changes of the intensity of an ordinary light beam $I_R(t)$ reflected from a crystal representing a Fabry-Perot interferometer with a temperature-dependent phase incursion. Smooth changes $U_{FP}(t) \sim I_R(t)$ for $0 < t < 74$ s occur in the heating cycle from the equilibrium state at room temperature $T_R \approx 24°$C to the heater temperature $T_h \approx 32°$C, as follows from Figure 2, *a*. It can be seen that the shielding charge is not reset from the polar surfaces up to the time $t \approx 75$ s, leading to a change of the intracrystalline field and, accordingly, the reflectance of the light beam from the crystal. However, the electrical discharge occurring at time $t \approx 75$ s leads to its rapid change.

The dynamics of $I_R(t)$ fluctuations in the natural cooling cycle of the crystal, which at a temperature of $T_h \approx 40°$C occurred at a rate of ~ 1 K/min (Figure 2, *b*), is characterized by sharp transitions between states with smooth behavior, with intervals between them from 5 to 30 s. The relative magnitude of the changes may exceed the value $|\Delta I_R|/I_R = 0.25$ in this case. It was found from experiments conducted at low sweep rates that such sharp jumps in the reflectance from the crystal are random and are observed both in the cycles of its heating and cooling.

A series of experiments was conducted with crystal heating and cooling at sweep rates from 500 ms/div to 1 μs/div to determine the time parameters and features of the observed abrupt changes of the reflectance from the crystal. Characteristic waveforms for $U_S(t)$ (dependencies *1*) and for $dU_S(t)/dt$ (dependencies *2*), recorded by the main channel and the synchronization channel at a sweep rate of 500 ms/div and 50 μs/div, are shown in Figures 3, *a* and 3, *b* respectively. These waveforms relate to two different experiments and were obtained for the cooling stage at $T_h \approx 35°$C (Figure 3, *a*) and heating stage at $T_h \approx 108°$C (Figure 3, *b*).

It can be seen from Figure 3, *a* that in this case a stepwise change of the reflectance from the crystal is not accompanied by the appearance of oscillations $U_{FP}(t) \sim I_R(t)$, however, the presence of such vibrations becomes noticeable in Figure 3, *b*, especially for a synchronization signal amplified by a transistor cascade. In some cases, abrupt changes of $I_R(t)$ lead to concomitant fluctuations with significant amplitude and a complex spectrum, which is illustrated by an oscillogram with a sweep rate of 1 ms/div in Figure 4, recorded at $T_h \approx 35^\circ$C for another experimental implementation of heating the crystal. The oscillation frequency range can be estimated from the oscillogram as 200–300 kHz. This makes it possible to assume that they are related to the shock piezoelectric excitation of longitudinal acoustic waves experiencing re-reflections from surfaces bounding a cylindrical sample of lithium niobate.

To estimate the characteristic transition time of a crystal representing a Fabry-Perot optical resonator between two states with different reflectances, we use relatively smooth oscillograms for $U_S(t)$, not accompanied by significant fluctuations, at sweep rates of 10, 5 and 1 μs/div, represented in Figure 5, *a, b* and *c*, respectively. Although they correspond to different temperature values T_h in the cooling cycles and relate to two separate experiments, their time dependences are qualitatively similar.

It follows from them that the duration of the edge for such a transition does not exceed the values $\tau_f = 1\,\mu$s. It is necessary to use a photodetector system for detecting laser radiation with higher performance for an accurate assessment of τ_f.

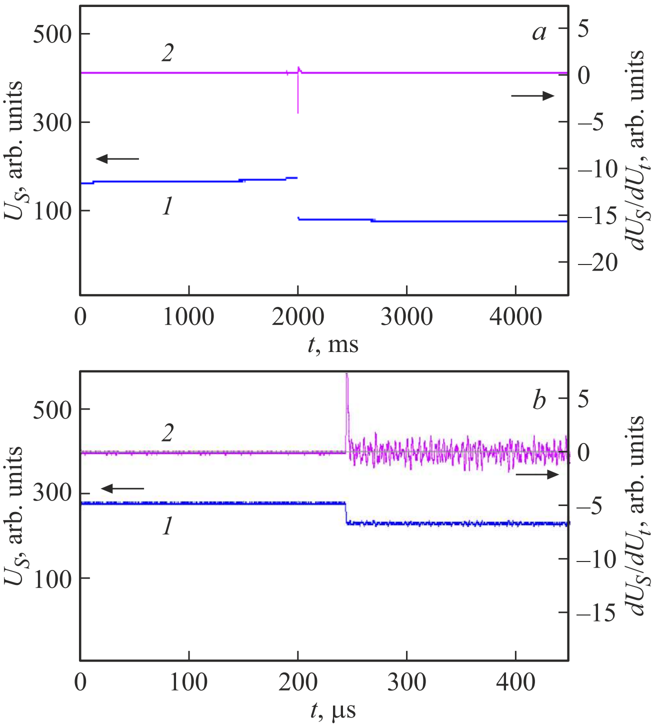

Figure 3. Time dependences of voltage (*1*) and its derivative (*2*) recorded at 500 ms/div (*a*) and 50 μs/div (*b*).

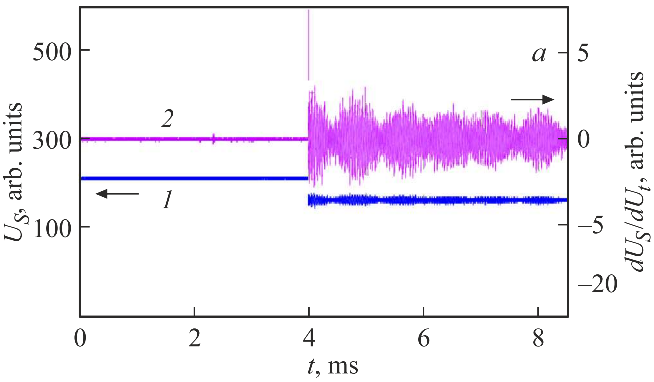

Figure 4. Time dependences of the voltage (*1*) and its derivative (*2*) recorded at sweep rate 1 ms/div.

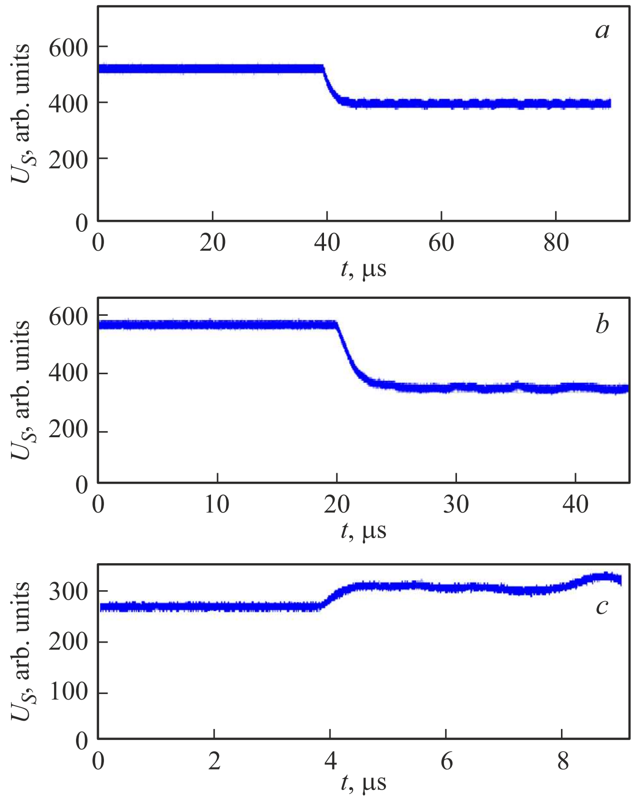

Figure 5. Time dependences of voltage and its derivative, recorded at a sweep rate 10 μs/div (*a*), 5 μs/div (*b*) and 1 μs/div (*c*).

4. Discussion of results

The time changes observed in the heating and cooling cycles for the reflectance of a laser beam from a lithium niobate crystal with parallel *Z*-faces forming a Fabry-Perot interferometer are attributable to variations of its ordinary refractive index $n_o(t)$ and thickness $h_{cr}(t)$ with temperature, $T(t) = T_R + \Delta T(t)$. The disturbances $n_o(t)$ associated with the thermo-optical (to) and pyroelectric (py) effects [14,15] can be divided as follows In the approximation of a homogeneous temperature distribution $T(t)$ over a crystal

$$\Delta n_o^T(\Delta T) = \Delta n_o^{to}(\Delta T) + \Delta n_o^{py}(\Delta T). \quad (1)$$

The thermo-optical contribution to changes of the refractive index over a limited temperature range is approximated by the linear function $\Delta n_o^T(\Delta T) = (dn_o/dT)\Delta T$, where the coefficient dn_o/dT can be found from the corresponding Selmeyer equations (see, for example, [16]). The pyroelectric component $\Delta n_o^{py}(\Delta T)$ for an open crystal is determined by an electric field, the intensity vector of which is directed along the polar axis Z, induced due to a change of spontaneous polarization with sufficiently rapid variations $\Delta T(t)$ [14]:

$$E_3^{py}(t) = -\frac{p}{\varepsilon_3}\Delta T(t), \tag{2}$$

where p is the pyroelectric coefficient and ε_3 is the static dielectric constant of the crystal for the field along the axis Z. The dependence of the pyroelectric component of perturbations of the ordinary refractive index on time is represented as follows using the known relations for the linear electro-optical effect in crystals of symmetry $3m$ [17]

$$\Delta n_o^{py}(t) = \frac{n_o^3 r_{13} p}{2\varepsilon_3}\Delta T(t), \tag{3}$$

where the temperature dependence is neglected for the electro-optical constant of the crystal r_{13}, as for other material parameters of lithium niobate.

In addition, relaxation processes of nonequilibrium perturbations Δn_o^{py} associated with a pyroelectrically induced electric field occur in the crystal. The slow relaxation, which can be described by some function Δn_o^{rel}, opposite in sign to $\Delta n_o^{py}(t)$, is attributable to the effect of compensation of the depolarizing field by the current of free charges in the crystal and in the surrounding air atmosphere [18] and does not lead, like thermal expansion, to any qualitative changes in the nature of the time dependence for the total phase incursion $\Delta\varphi^T(t)$ of the light beam in the Fabry-Perot interferometer. Neglecting the contributions of these processes and taking into account the above relations, we obtain

$$\Delta\varphi^T(t) = \frac{4\pi h_{cr}}{\lambda}\left[\frac{dn_o}{dT} + \frac{n_o^3 r_{13} p}{2\varepsilon_3}\right]\Delta T(t). \tag{4}$$

It should be noted that under the conditions of the experiments, temperature changes of the size of a cylindrical crystal free from external elastic stresses were ensured both along the polar axis Z and in the radial direction (see Figure 1). The absence of elastic stresses associated with radial elastic displacements is attributable to the coefficient of linear thermal expansion of the dielectric insert (*2*) exceeding the corresponding coefficient $\alpha_a = 14.1 \cdot 10^{-6}$ 1/K of lithium niobate [19]. Any significant temperature gradients occurring during heating and cooling cycles in a crystal, as is known [20], should not lead to any significant effect of the tertiary effect on the generated pyroelectric field due to such conditions of free size changes.

Let us describe the experimentally observed smooth dependence $U_S(t)$, shown in Figure 2, *a* for the time interval $0 < t \le t_d$, where $t_d = 75$ s by using the following model, taking into account (4), the above-described features of the experimental technique and the known ratios [21]

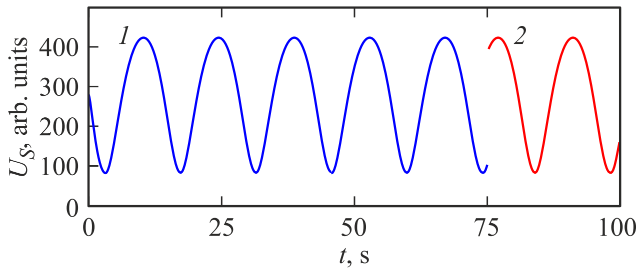

Figure 6. Time dependences for the recorded voltage, calculated using the formula (5) for the interval $0 \le t \le 75$ s (curve *1*) and at $t > 75$ s (curve *2*).

for the reflectance of light radiation from the Fabry-Perot interferometer:

$$U_S(t) = U_0 + U_m$$
$$\times \frac{4R_o \sin^2\left[\frac{2\pi h_{cr}}{\lambda}\left(\frac{dn_o}{dT} + \frac{n_o^3 r_{13} p}{2\varepsilon_3}\right)\Delta T(t) - \frac{n_o^3 r_{13}}{2}\Delta E(t)\right]}{(1-R_o)^2 + 4R_o \sin^2\left[\frac{2\pi h_{cr}}{\lambda}\left(\frac{dn_o}{dT} + \frac{n_o^3 r_{13} p}{2\varepsilon_3}\right)\Delta T(t) - \frac{n_o^3 r_{13}}{2}\Delta E(t)\right]}, \tag{5}$$

where $R_o = \left[(n_o - 1)/(n_o + 1)\right]^2$ is the reflectivity of Z-crystal faces. The results of calculating the smooth time dependence $U_S(t)$ for the time interval $0 \le t \le 75$ s, shown in Figure 6 of the curve *1*, obtained using the thermo-optical constant $dn_o/dT = 1.165 \cdot 10^{-5}$ 1/K [16] and the pyroelectric coefficient $p = -10.39 \cdot 10^{-5}$ C/(m^{2}K) [14] for congruent lithium niobate, as well as its following material parameters in a mechanically free state: $\varepsilon_3 = 2.543 \cdot 10^{-10}$ F/m [22] and $r_{13} = 11.3 \cdot 10^{-12}$ m/V [23]. It was assumed at this time interval for the qualitative agreement of the calculation according to the formula (5) with the corresponding experimental data presented above in Figure 2, *a*, that $U_0 = 80$, $U_m = 720$; the initial crystal temperature $T_R = 24.09$°C, and its increment is realized at a constant rate of 0.089 K/s from the initial value $\Delta T = 0.91$ K.

A comparison of the dependences in Figure 2, *a* and Figure 6 shows that the model used allows for a satisfactory description of the variations observed at the initial stage of heating of a pyroelectric lithium niobate crystal with the temperature of its ordinary refractive index. The crystal temperature increases by 7.6 K during the specified time for the accepted conditions and the material parameters used, and the pyroelectrically induced field in the crystal reaches the value $E_3^{py}(t_d) \approx -31$ kV/cm. The intensity of the electric field $E_G(t_d)$ created in this case in a gap with a size of h_g between the upper face of the crystal (*1*) and the anode (*5*) (see Figure 1), can be approximated from the ratio [24]

$$E_G(t_d) = \frac{p\Delta T(t_d)}{h_g \varepsilon_3/h_{cr} + \varepsilon_0}, \tag{6}$$

where ε_0 is an electrical constant. The gap $h_g = 10$ mm corresponds to the value $E_G(t_d) \approx -36$ kV/cm, which may be overestimated because of the differences of the material parameters of the studied lithium niobate crystal from those used in the estimated calculations. It is characteristic that it exceeds the air breakdown voltage at atmospheric pressure. Assuming that the recorded rapid changes of $U_S(t)$ at $t > t_d$ are associated either with a breakdown of the gap between the translucent anode and the upper face of the crystal, or with another type of breakdown, for example, along its lateral surface between Z-faces, from (5), the decrease of the absolute magnitude of the electric field in the crystal can be estimated as $|\Delta E_3(t_d)| \approx 4$ kV/cm. The surface charge on the crystal faces accordingly decreases by $|\Delta\xi(t_d)| \approx 23$ nC with such a pyroelectrically induced electric discharge, assuming the uniform distribution of this surface charge over the area $S \approx 2.3 \cdot 10^{-4}\,\mathrm{m}^2$. It should be noted that this value is in order of magnitude agreement with estimates of the transferred charge, which reaches 5.7 nC during pyroelectric generation of a pulsed electron beam with currents up to 600 mA, recorded at atmospheric pressure in a coaxial configuration device for a cylindrical crystal of lithium niobate with similar dimensions [13].

The dynamics of changes of the intensity of the beam $I_R(t) \sim U_{FP}(t)$ reflected from the crystal experimentally observed after an electric discharge at $t > 75$ s (Figure 2, *a*) is no longer described within the framework of the considered simple model: the values in the minima remain the same as before the discharge for dependence $U_S(t)$ calculated by the formula (5) and the curve shown in Figure 6 *2*. The reason for the increase of minima over time for $U_S(t)$, smooth before the electric discharge, and abrupt after it, requires study. An additional factor complicating the behavior of $I_R(t)$ may be the photorefractive effect, which to the formation of reflective holograms leads in crystals of Z-orientations with parallel faces that increase or decrease the transmission of the probing beam, depending on the orientation of the polar axis [25].

5. Conclusion

Thus, the presented technique for recording the dynamics of the electric field in a lithium niobate crystal with parallel Z-faces in case of pyroelectric generation of electric discharges made it possible to display its time dependences during the intervals from ~ 90 s to $\sim 9\,\mu$s. The jumps of the intensity of the pyroelectrically induced electric field observed in the cycles of heating and cooling of the crystal, reaching values of 4 kV/cm, demonstrate the behavior characteristic of electric discharges. The surface charge on the crystal faces decreases by an amount that can be units of nC in this case, with the duration of the discharge process not exceeding $1\,\mu$s. It was found that in case of some electric discharges, a sharp decrease of the electric field strength in the crystal causes fluctuations of the intensity of the laser beam reflected from it with a significant amplitude and a complex spectrum in the frequency range from 200 to 300 kHz. It is suggested that these fluctuations are related to shock piezoelectric excitation of longitudinal acoustic waves experiencing re-reflections from surfaces bordering a cylindrical lithium niobate sample.

Acknowledgments

The authors would like to thank V.F. Tarasenko and P.V. Karataev for useful discussions.

Funding

The study was financially supported by the Ministry of Science and Higher Education of the Russian Federation as part of the state assignment for 2023–2025 (FEWM-2023-0012).

Conflict of interest

The authors declare that they have no conflict of interest.

References

[1] G. Rosenman, D. Shur, Ya.E. Krasik, A. Dunaevsky. J. Appl. Phys. **88**, *11*, 6109 (2000).
[2] B. Naranjo, J.K. Ginzewski, S. Putterman. Nature (London) **434**, 1115 (2005).
[3] W.T. Arkin. Trends in Lasers and Electro-Optics Research / Editor W.T. Arkin. Nova Science Publishers (2006). P. 59.
[4] E.M. Bourim, C.W. Moon, S.W. Lee, V. Sidorkin, I.K. Yoo. J. Electroceram **17**, 479 (2006).
[5] J.A. Geuther, Y. Danon. Appl. Phys. Letters **90**, *17*, 174103 (2007).
[6] E.L. Neidholdt, J.L. Beauchamp. Anal. Chem. **79**, *10*, 3945 (2007).
[7] N.V. Kukhtarev, T.V. Kukhtareva, G. Stargell, J.C. Wang. J. Appl. Phys. **106**, 014111 (2009).
[8] http://www.amptek.com/coolx.html. Amptek Inc., Miniature X-ray generator with pyroelectric crystal.
[9] V.A. Andrianov, A.A. Bush, A.L. Erzinkyan, K.E. Kamentsev. Poverkhnost. Rentgen., sinkhrotron. i nejtron. issled. *7*, 25 (2017). (in Russian).
[10] M. Wilke, L. Hanns, K. Harnisch., W. Knapp, M. Ecke, T. Halle. IOP Conf. Ser. Mater. Sci. Eng. **882**, *1*, 012026 (2020).
[11] M. Ali, P. Karataev, A. Kubankin, A. Oleinik. Nucl. Instrum. Methods Phys. Res. A **1061**, 169134 (2024).
[12] M.J. Johnson, J. Linczer, D.B. Go. Plasma Sources Sci. Technol. **23**, 065018 (2014).
[13] K.M. Mambetova, S.M. Shandarov, S.I. Arestov, L.N. Orlikov, A.A. Elchaninov, N.I. Burimov, A.I. Aksenov. J. Instrum. **17**, P04008 (2022).
[14] J. Parravicini, J. Safioui, V. Degiorgio, P. Minzioni, M. Chauvet. J. Appl. Phys. **109**, 033106 (2011).
[15] S.T. Popescu, A. Petris, V.I. Vlad. J. Appl. Phys. **113**, *4*, 043101 (2013).
[16] V.G. Dmitriev, G.G. Gurzadyan, D.N. Nikogosyan. Handbook of nonlinear optical crystals. Springer, Berlin 64, (2013). 414 p.
[17] Yu.I. Sirotin, M.P. Shaskolskaya, Fundamentals of Crystallophysics. Nauka, M. (1979). 640 p. (in Russian).

[18] M. Lines, A. Glass. Segnetoelektriki i rodstvennye im materialy / Pod red. V.V. Lemanov and G.A.Smolensky. Mir, M. (1981). 736 p. (in Russian).
[19] T. Volk, M. Wöhlecke. Lithium niobate: defects, photorefraction and ferroelectric switching. Springer, Berlin 115, (2008). 258 p.
[20] K.M. Nurieva, A.K. Tagantsev, V.A. Trepakov, V.M. Varikash. FTT **31**, *1*, 130 (1989). (in Russian).
[21] M. Born, E. Wolf. Osnovy optiki. Nauka, M. (1973). 719 p. (in Russian).
[22] R.T. Smith, F.S. Welsh. J. Appl. Phys. **42**, 2219 (1971).
[23] M. Luennemann, U. Hartwig, G. Panotopoulos, K. Buse. Appl. Phys. B **76**, 403 (2003).
[24] T.Z. Fullem, Y. Danon. J. Appl. Phys. **106**, 074101 (2009).
[25] I.F. Kanaev, V.K. Malinovsky, B.I. Sturman. ZhETF **74**, *5*, 1599 (1978). (in Russian).

Translated by A.Akhtyamov